INTRODUCTION

1. The urgency of the thesis

The automobile industry in Vietnam has produced a number of assembly sheets such as cabs, trunks, chassis, tires, carcasses, plastic, rubber but has not manufactured assemblies of power transmission system such as gearboxes, propeller shafts, driving axles, which must be imported 100% from overseas.

In-depth research using scientific theory is a necessity to gradually develop applications into practical production. In our country, there are no researches on the effect of the dynamic parameters of the durability of propeller shaft.

2. Research objective

To build the basis for the research of kinetics, dynamics and the durability of propeller shaft with specific objects and results which can be applied in research and practice for the manufacture of propeller shaft of trucks and whereby expanding to other automotive assemblies.

3. Research subject

The research subject is the assembly of propeller shaft in the powertrain of trucks with load of up to 3 tons.

4. Research scope and limitation

Propeller shaft in light trucks with load of up to 3 tons LF3070G1 type assembled in Vietnam;

The influence of some design parameters and structural changes of the propeller shaft such as length, thickness, inclination of the shaft in the vertical plane, the influence of rotational inertia at both shaft ends on dynamics, stress, deformation and durability of the researched subject.

Ignore the rotational friction at both ends of the universal joints and spline tube on the propeller shaft.

5. Scientific and practical significance

5.1 Scientific significance

The scientific significance of the thesis has developed a research methodology for the durability of propeller shaft; built the differential equations of the motion of cardan universal joints as well as the equations of motion and kinetics of propeller shaft according to the dynamics of multi-body system as the basis for the design of cardan shaft, constructed a finite element model to investigate the influence of dynamic parameters on the durability of propeller shaft; including:

- Building the equation describing the motion of cardan universal joints and propeller shaft. Solving differential equation of motion and simulating dynamics of the assembly by using Matlab Mupad and Simunlink software.
- Using finite element method with ANSYS Workbench software as a simulation tool for the survey of the durability of propeller shaft.
- Developing experimental method to specify dynamic parameters; Designing an experimental platform and wireless transceiver to receive signals from the rotating propeller shaft.

5.2 Practical significance

Studying kinetics and dynamics and the durability of propeller shaft in trucks, applying to the design, new fabrication and improvement of durability, replacement of propeller shaft.

Designing experimental platform of propeller shaft with wireless transceiver created to determine the influences of three dynamic parameters (torque, stress, number of revolution) on the durability of propeller shaft. The experimental platform can be applied in practical production and the evaluation of the shaft quality.

The research outcomes of the thesis can be used as reference material for in-depth and extended studies within training and research institutes, as well as for the process of design calculation of propeller shaft.

6. Research methodology

6.1 Research on theory

Research on the kinematic theory of propeller shaft.

- Studying the theory of dynamics of propeller shaft.
- Studying the theory of durability of propeller shaft.
- Analyzing the working mode of propeller shaft in trucks with load of up to 3 tons produced and assembled within the country.
- Executing numerical stimulation and survey on the kinetics and dynamics of propeller shaft.
- Executing numerical stimulation and survey on the durability of propeller shaft.

6.2 Experimental research
- Experimental research evaluates the quality of propeller shaft by using the thesis of manufacturing experimental platform and wireless signal transceiver to measure the parameters of rotating propeller shaft with kinetic and dynamic factors, durability of the propeller shaft in light trucks.
- Testing on the experimental platform: collect the data of kintetic and dynamic parameters and durability of propeller shaft.

7. New contributions of the thesis
- Develop a spatial model, establish dynamic equation of the assembly of propeller shaft in the powertrain of the trucks with load of up to 3 tons by kinetics and dynamics of multi-body system;
- Use the Matlab Mupad, Simulink and Ansys Workbench software which are powerful specialized tools for studying some dynamic parameters of propeller shaft, the results of which are the scientific basis of the calculation of propeller shaft durability;
- Establish experimental methods to identify some dynamic parameters and the durability of propeller shaft;
- Design and manufacture the experimental platform for the open power test with modern and standard equipment;
- Design and manufacture of wireless signal transceivers to receive signals from the rotating propeller shaft by non-destructive signal reception;
- Measure the deformation value from the transfer of non-electrical signals to electrical signals, digital signals and identify the specific measurement value through the calibration on the direct stress machine and wireless signal transceiver.

8. Thesis content
Introduction
Chapter 1: Overview of research issues
Chapter 2: Identification of dynamic parameters and the durability of propeller shaft
Chapter 3: Survey on the influences of dynamic parameters on the durability of propeller shaft
Chapter 4: Experimental research
Conclusion and further research direction

Chapter 1
OVERVIEW OF RESEARCH ISSUES

1.1 Overview of automobile industry in Vietnam

In the automobile industry, trucks account for a large proportion of the market share which meet the demand of goods transportation and suitable production for urban and rural areas. When the need for trucks is increasing more and more, it is necessary to use auxiliary parts which are mostly imported from foreign countries at a high cost. Research and development of high quality products are essential for the self-production of complete assemblies assisting the automotive manufacturing and assembling industry within the country. Among those, the top priority is in-depth research for design and manufacture of automotive assemlies and of the powertrain in which manufacture of propeller shaft is one of the most important tasks of Vietnam industry in the current period.

1.2 Overview of propeller shaft in trucks

Propeller shaft in the powertrain is used to transmiss power from the gearbox to the rear axle drive of the vehicle. In addition to power transmission, it ensures the transmission of rotation between non-right angled shafts and transmission of torque between shafts which are not on the same line, but intersect at an α angle . Cardan universal joints are often subjected to large impact, while propeller shaft is twisted or bent by the collision and the spline surface on the propeller shaft is also vulnerable to wear and tear, therefore power transmission of the propeller shaft must satisfy the requirements of power transmission, fabrication design, assembly and repair.

1.3 Classification of propeller shafts

Propeller shafts are categorized according to the use of power transmission, universal joints, kinematic features and structure of propeller shaft.

1.4 Analysis of propeller shaft structure in light truck

The propeller shaft structure in light trucks is presented in figure 1.1
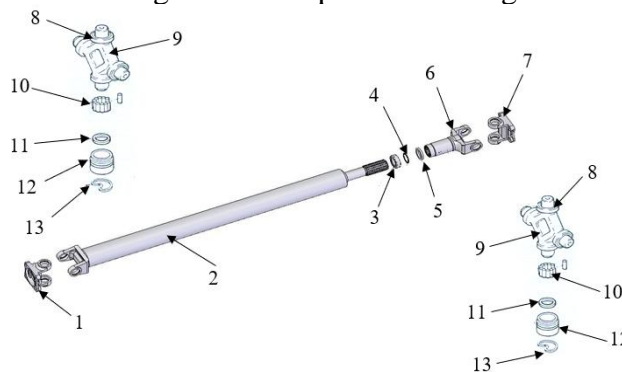
Figure 1.1 Main structure of propeller shaft in light truck
1. Cardan fork, 2. Long body, 3. Oil seal, 4. Retaining ring, 5. Nut, 6. Short body, 7.
Cardan fork, 8. Gasket, 9. Universal Joints, 10. Needle bearing, 11. Grease seal, 12. Needle
bearing cup, 13. Brake.

Propeller shaft must be dynamically balanced to minimize the vibration when working. If the transmission system has two shafts, dynamic balancing must be made simultaneously for both shafts. During dynamic balancing, it is necessary to weld metal pieces onto the body of the propeller shaft at the imbalance position to create counterpoise.

1.5 Some issues in the technology of manufacturing propeller shaft

Manufacturing method: cardan fork is moulded and processed, spline joint is made of steel 45, shaft body is made of steel pipe, universal shaft is made of alloy steel and forged. Check the oscillation balance of propeller shaft with specialized equipment, such as digital HOMMELWERKE GMBH's "Hommel Measuring Computer Family - MC20" with 3D analysis devices and data analysis and processing softwares, material analysis devices.

1.6 Typical damages of propeller shaft

During operation, due to the occurrence of the highest stresses on the propeller shaft assembly, micro cracks are formed and progressively developed, along with the oscillation of the forces on the shaft which expand the cracks. The occurrence of force on such conditions causes greater stresses compared to the allowable stress of the material which makes the durable limit overpass the plastic deformation area. The load bearing process takes place continually and repeatedly, causing damages to the parts of the propeller shaft.

Some typical damages: wear of shaft collars on U-bolt(a); wear on bearings (b); wear on bolt collar (c); wear on U-bolt collar (d); break of U-bolt (e).

Figure 1.2: Typical damages of propeller shaft

1.7 The research situation of propeller shaft on international and domestic scale
1.7.1 Research situation in the world
There are some remarkable research projects which are independent and academic works, but no practical research for the application to actual production.
1.7.2 Research situation in our country
Researches on propeller shaft mainly focus on kinetics, dynamics and the balance of propeller shaft in the form of teaching materials in universities and colleges.
On domestic scale, almost studies on automotive propeller shaft are at the level of research for training purpose, and there is no in-depth research for practical application in order to replace imported products.

CONCLUSION OF CHAPTER 1

Presenting comprehensive studies of the domestic automobile manufacture and assembly market as well as the demand and situation of manufacturing localized products. Generalizing the development of the automobile industry and the actual demand for the localization of automobile parts and components, specifically the localized production of propeller shaft assembly from design to manufacture.
From the overview research, international and domestic research projects, the author of the thesis has defined the mission, purpose, methodology and content of the research to contribute to the localization of the domestic automobile industry, support the scientific research and training.
Building the basis for the research methodology of kinetics, dynamics and the durability of propeller shaft which can be applied in research and in practical production.
Proposing the objective of the extended and in-depth research thesis focusing on the propeller shaft assembly in trucks and based on which to extend to other objects in the manufacture of automotive assemblies.

Chapter 2
IDENTIFICATION OF DYNAMIC PARAMETERS AND THE DURABILITY OF PROPELLER SHAFT

2.1 Modelling dynamics of multi-body system of propeller shaft in power transmission system.
Propeller shaft model in the powertrain of light trucks is a mechanical system consisting of five solid parts linked together shown in Figure 2.1
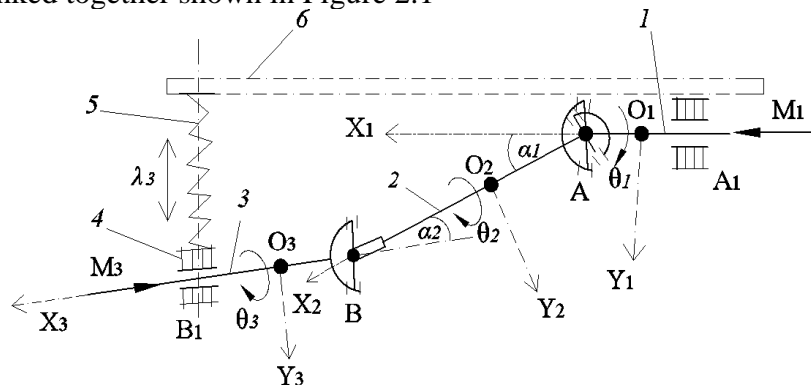

Figure 2.1 Mechanical diagram of propeller shaft in light trucks

When the angle of the deflection angles of shaft 1 and 3 is constant during the motion (α_1, α_1 = const), shaft 1, 2 and 3 only rotate around their own shafts.
The objects are defined as follows:
Object 1 (Driving shaft (front cardan fork)) with weight concentrated at the focal point O_1 and object coordinate system $O_1X_1Y_1$, generalized coordinates θ_1 and torque M_1
Object 2 (Front universal) with weight concentrated at the focal point A and object coordinate system AX_AY_A, generalized coordinates ψ_1 and torque τ_1

Object 3 (Shaft body) with weight concentrated at the focal point O_2 and object coordinate system $O_2X_2Y_2$, generalized coordinates θ_2 and torque M_2

Object 4 (Rear universal) with weight concentrated at the focal point B and object coordinate system BX_BY_B, generalized coordinates ψ_2 and torque τ_2

Object 5 (Driven shaft (rear cardan fork)) with weight concentrated at the focal point O_3 and object coordinate system $O_3X_3Y_3$, generalized coordinates θ_3 and torque M_3

Providing the dimensions as: $AO_1=a_1$, $AO_2=a_2$, $BO_3=a_3$, $AB=L$ (L is the length of propeller shaft. The thesis studies on 3 cases: L1 = 1450mm, L2 = 1300mm, L3 = 1150mm)

2.2 Building equation of dynamics of multi-body system of propeller shaft

Full generalized coordinates of the system

Apply the Lagrange equation of 2nd type we have:

$$\frac{d}{dt}\left(\frac{\partial L}{\partial \dot{q}_j}\right) - \frac{\partial L}{\partial q_j} = Q_j \tag{2.1}$$

Where: L is the Lagrange function defined by L = T-V (in case potential energy is unchanged, L = T); T is the kinetic energy of the system; q_j is generalized coordinates of the system (in this case $q_j = \psi_i$); Q_j is the generalized force of the system (in this case $Q_j = \tau_i$).

The full generalized coordinates are:

$$\tag{2.2}$$
$$q = [\varphi_1, \varphi_2, \varphi_3, \psi_1, \psi_2]^T$$

Where: θ_1 - Angular displacement of driving shaft 1; θ_2 - Angular displacement of propeller shaft 2; θ_3 - Angular displacement of driven shaft 3; ψ_1 - Angular displacement of front universal shaft; ψ_2 - Angular displacement of rear universal shaft.

Case 1: No consideration of the inertial mass of the universal shaft

The full generalized coordinates in this case are:

$$q = [\theta_1, \theta_2, \theta_3]^T \tag{2.3}$$

Based on the calculation of mass moment of inertia, direction cosine matrix, barycentric coordinates and Jacobi norms of translation of objects, angular velocity and Jacobi determinant of rotation of objects, mass matrix, the system's kinetic energy, potential energy, the dissipation function of the system, generalized force, we can build up the differential equation of motion of the powertrain as follows:

$$I_1\ddot{\theta}_1 + c_x\left(\theta_1 - \theta_{31}\right) + k_x\left(\dot{\theta}_1 - \dot{\theta}_{31}\right) = M_1 \tag{2.4}$$

$$I_2\left(2cos^2\alpha_1 - 1\right)\ddot{\theta}_2 = 0 \tag{2.5}$$

$$I_3\left(2cos^2\alpha_{31} - 1\right)\ddot{\theta}_3 - c_x\left(\theta_1 - \theta_{31}\right) - k_x\left(\dot{\theta}_1 - \dot{\theta}_{31}\right) = -M_3 \tag{2.6}$$

Hence:

+ If $\alpha_{31} = 0$, or $\alpha_1 = -\alpha_2$ (shaft 1 and 3 are parallel), the differential equation system (2.4, 2.5, 2.6) is built as:

$$I_1\ddot{\theta}_1 + c_x\left(\theta_1 - \theta_3\right) + k_x\left(\dot{\theta}_1 - \dot{\theta}_3\right) = M_1 \tag{2.7}$$

$$I_2\left(2cos^2\alpha_1 - 1\right)\ddot{\theta}_2 = 0 \tag{2.8}$$

$$I_3\ddot{\theta}_3 + c_x\left(\theta_1 - \theta_{31}\right) + k_x\left(\dot{\theta}_1 - \dot{\theta}_{31}\right) = -M_3 \tag{2.9}$$

+ The above differential equations established with the assumption that α_1, α_2 and α_{31} are constants. But when the vehicle operates in reality, these angles are different over time, depending on the distortion of the rear axle spring (λ). It means when solving an equation system (2.7, 2.8, and 2.9) we must consider that:

$$\alpha_i = \alpha_i(\lambda) \text{ With } \lambda = \lambda(h_b, t)$$

5

To identify $\lambda(h_b, t)$ we must solve the oscillation math of rear axles when driving cars on bumpy roads.

+ After surveying the differential equation system (2.7, 2.8, 2.9) we should find the torsion angle of shaft 2 according to the formula (2.10).

$$\theta_2 = \theta_{31} - \theta_1 \tag{2.10}$$

Case 2: Consideration of the inertial mass of the universal shaft

Studying kinetics, dynamics of propeller shaft assembly in case of the impact of universals. The parameters $\dot\theta_2, \dot\psi_3$ are calculated to $\theta_1, \dot\theta_1$ and $\theta_4, \psi_5, \dot\theta_4, \dot\psi_5$ to $\theta_1, \dot\theta_1$. The function of kinetic energy calculated to 2 variables θ_1 and $\dot\theta_1$ in form of $T(\theta_1, \dot\theta_1)$.

Using scalar product and vector product formulas and other calculation formulas, we have the equation:

$$\sin\psi_3 = \frac{1}{\sqrt{1 + \cot g^2\psi_3}} \quad \text{and} \quad \cot g\psi_3 = -tg\psi_1\cos\alpha \tag{2.11}$$

$$\cos\theta_2 = \frac{1}{\sqrt{1 + \cos^2\alpha.tg^2\psi_1}}\left(\sin\alpha\cos\psi_1 + \cos\alpha\sin\psi_1 tg\psi_1\right) \tag{2.12}$$

The equations (2.11, 2.12) describe dynamic parameters and angular displacement of propeller shaft (ψ_3), U-joint (θ_2) in relation with angular displacement of driving shaft (ψ_1)

2.3. Angular momentum of propeller shaft assembly:

Define the angular momentum of driving shaft, angular momentum of propeller shaft joint, angular momentum of driven shaft to identify the kinetic energy of each part in the fixed coordinate system $O_0 x_0 y_0 z_0$, through which determine the total kinetic energy of propeller shaft assembly according to the equation (2.13).

$$T = \frac{1}{2}\left(I_1^{zz} + s^2(\theta_2)I_2^{xx} + c^2(\theta_2)I_2^{yy}\right)\dot\psi_1^2 + \frac{1}{2}I_2^{zz}\dot\theta_2^2 + \tag{2.13}$$

$$+ \frac{1}{2}\left(I_3^{yy} + s^2(\theta_4)I_4^{xx} + c^2(\theta_4)I_4^{yy}\right)\dot\psi_3^2 + \frac{1}{2}I_4^{zz}\dot\theta_4^2 + \frac{1}{2}I_5^{yy}\dot\psi_5^2$$

2.4 Analysis of dynamic parameters of propeller shaft in Matlab Mupad program:

2.4.1 Kinetic energy of the system

Run the Mupad program in Matlab to receive the result of kinetic energy on propeller shaft.

2.4.2 Angular displacement and angular velocity on objects

Providing: $\alpha = a$; $\beta = b$; $\omega_l = \theta_l$, where ω_l is angular velocity on shaft 1, we have the result of angular displacement as follows:

$$\theta_2 = \arccos\left(\frac{\sin(a)\sin(t_1) + \dfrac{\cos(a)\cos(t_1)}{\tan(t)}}{\sqrt{\dfrac{\cos(a)^2}{\tan(t_1)} + 1}}\right) \tag{2.14}$$

$$\dot\theta_2 = \frac{\omega_1\left(\dfrac{\dfrac{\cos(\alpha)\sin(\theta_1)}{\tan(\theta_1)} - \cos(\theta_1)\sin(\alpha) + \dfrac{\cos(\alpha)\cos(\theta_1)\sigma_3}{\tan(\theta_1)^2}}{\sqrt{\sigma_1}} - \dfrac{\cos(\alpha)^2\sigma_3\sigma_2}{\tan(\theta_1)^3\sigma_1^{3/2}}\right)}{\sqrt{1 - \dfrac{\sigma_2^2}{\sigma_1}}} \tag{2.15}$$

$$\theta_3 = -\arctan\left(\frac{\tan(\theta_1)}{\cos(\alpha)}\right) \tag{2.16}$$

$$\dot\theta_3 = -\frac{\omega_1(\tan(\theta_1)^2 + 1)}{\cos(\alpha)\left(\dfrac{\tan(\theta_1)^2}{\cos(\alpha)^2} + 1\right)} \tag{2.17}$$

$$\theta_3 = \arccos\left(\frac{\sin(\alpha)\sin(\theta_3) + \dfrac{\cos(\alpha)\cos(\theta_3)}{\tan(\theta_3)}}{\sqrt{\dfrac{\cos(\alpha)^2}{\tan(\theta_3)^2} + 1}}\right)$$

(2.18)

$$\dot{\theta}_4 = \frac{\dfrac{\omega_1\left(\dfrac{\sigma_2}{\sigma_5^{3/2}} - \dfrac{\sin(\alpha)\sigma_2}{\sigma_4} + \dfrac{\cos(\alpha)^2\sigma_2}{\tan(\theta_1)^2\sqrt{\sigma_5}}\right) + \dfrac{\sin(\alpha)\tan(\theta_1)^2\sigma_2}{\cos(\alpha)^3\sigma_5^{3/2}}}{\sqrt{\sigma_1}} - \dfrac{\cos(\alpha)^4\sigma_3\sigma_2}{\tan(\theta_1)^3\sigma_1^{3/2}}}{\sqrt{1 - \dfrac{\sigma_3^2}{\sigma_1}}}$$

(2.19)

$$\theta_5 = -\arctan\left(\frac{\tan(\theta_3)}{\cos(\beta)}\right)$$

(2.20)

$$\dot{\theta}_5 = \frac{\omega_1(\tan(\theta_1)^2 + 1)}{\cos(\alpha)\cos(\beta)\left(\dfrac{\tan(\theta_1)^2}{\cos(\alpha)^2\cos(\beta)^2} + 1\right)}$$

(2.21)

2.4.3 Building dynamic equation for the whole system

The motion equation of propeller shaft system is built as follows:

$$\gamma_1\left(1.0I_2^{xx}\sigma_8 - 1.0I_1^{zz} + \frac{1.0I_4^{zz}\sigma_3^2}{\sigma_{15}} - \frac{1.0I_2^{yy}(\sigma_{25} + \sigma_{23})^2}{\sigma_{31}} + \frac{1.0I_2^{zz}\sigma_7^2}{\sigma_8} - \frac{1.0I_3^{yy}\sigma_{30}^2}{\sigma_9} + \right.$$

$$\left. + \frac{1.0\sigma_4\sigma_{30}^2}{\sigma_9} - \frac{1.0I_5^{yy}\sigma_{30}^2}{\sigma_{10}}\right) - \omega_1\left(1.0\omega_1\sigma_6 + \frac{1.0\omega_1\sigma_{30}^2\sigma_2}{\sigma_9} - \frac{1.0\omega_1I_2^{zz}\sigma_{16}\sigma_7^2}{\sigma_8^2} + \right.$$

$$+ \frac{2.0\omega_1I_4^{zz}\sigma_3\sigma_1}{\sigma_{15}} - \frac{1.0\omega_1I_4^{zz}\sigma_{13}\sigma_3^2}{\sigma_{15}^2} - \frac{2.0\omega_1I_2^{zz}\sigma_7\sigma_5}{\sigma_8} + \frac{4.0\omega_1I_3^{yy}\tan(\theta_1)\sigma_{30}^2}{\sigma_9} -$$

$$- \frac{4.0\omega_1I_3^{yy}\tan(\theta_1)\sigma_{30}^3}{\sigma_{11}} + \frac{4.0\omega_1\tan(\theta_1)\sigma_4\sigma_{30}^2}{\sigma_9} + \frac{4.0\omega_1\tan(\theta_1)\sigma_4\sigma_{30}^3}{\sigma_{11}} -$$

$$- \frac{0.5\omega_1^2I_2^{zz}\sigma_{16}\sigma_7^2}{\sigma_8^2} + \frac{1.0\omega_1^2I_4^{zz}\sigma_3\sigma_1}{\sigma_{15}} - \frac{0.5\omega_1^2I_4^{zz}\sigma_{13}\sigma_3^2}{\sigma_{15}^2} +$$

$$+ \frac{2.0\omega_1^2I_3^{xx}\tan(\theta_1)\sigma_{30}^2}{\sigma_9} - \frac{2.0\omega_1^2I_3^{xx}\tan(\theta_1)\sigma_{30}^3}{\sigma_{11}} -$$

$$- \frac{2.0\omega_1^2\tan(\theta_1)\sigma_4\sigma_{30}^2}{\sigma_9} + \frac{2.0\omega_1^2\tan(\theta_1)\sigma_4\sigma_{30}^3}{\sigma_{11}} +$$

$$+ \frac{2.0\omega_1^2I_5^{yy}\tan(\theta_1)\sigma_{30}^2}{\sigma_{10}} - \frac{2.0\omega_1^2I_5^{yy}\tan(\theta_1)\sigma_{30}^3}{\sigma_{12}} = \tau_0$$

(2.22)

The coefficients of the equation are defined based on the kinetic parameters of propeller shaft specified in the appendix of the thesis.

2.5 Calculation parameters of the durability of propeller shaft

2.5.1 Durability of propeller shaft body

Propeller shaft dimensions are defined by the number of rotation nt of the propeller shaft. When calculating, we need to test the durability of the propeller shaft according to torsion, traction, compression and bending (when the shaft is subjected to horizontal oscillation). The calculated dimensions of the shaft body specified in Figure 2.8, including cardan front fork 1, cardan rear fork 3, 2-weld shaft body with spline tube at the welded position number 4. The dimensions are used for the below cases:

Case 1: Length $L_1 = 1450$mm, Thickness of the body $b_1 = 6$ mm
Case 2: Length $L_1 = 1450$mm, Thickness of the body $b_2 = 4$ mm
Case 3: Length $L_2 = 1300$mm, Thickness of the body $b_1 = 6$ mm
Case 4: Length $L_2 = 1300$mm, Thickness of the body $b_2 = 4$ mm
Case 5: Length $L_3 = 1150$mm, Thickness of the body $b_1 = 6$ mm
Case 6: Length $L_3 = 1150$mm, Thickness of the body $b_2 = 4$ mm
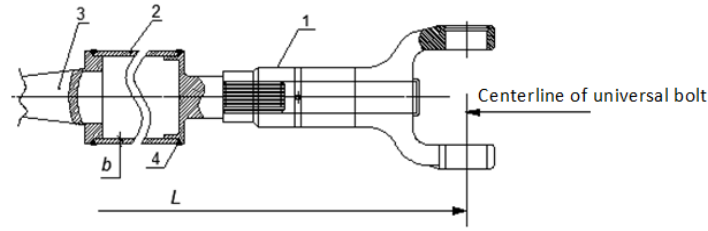
Figure 2.8 Calculation dimensions of shaft body

The body of propeller shaft is calculated by torsional stress:

$$\tau' = \frac{(\varphi_1 - \varphi_2)DG}{2L} \quad (MN/m^2)$$

And torsion angle of the propeller shaft θ:

$$\theta = \frac{180}{\pi} \cdot \frac{M_{e\,max}i_{h1}i_{p1}l}{GJ_x}K_d \quad (rad) \tag{2.23}$$

J_x – moment of inertia of cross section during torsion

D – External diameter of the propeller shaft (m)

L – Calculated length of the shaft (m)

G – Elastic modulus when moving (G = $0,8.10^5$MN/m^2).

2.5.2 The durability of U-bolts

U-bolt is calculated by bending, cutting, bearing with load P

$$P = \frac{M_{e\,max}i_{h1}i_{p1}}{2rc\cos\alpha}$$

U-bolt of the U-joint is calculated by bearing according to Formula (2.24).

$$\sigma_{cd} = \frac{\sqrt{2}P}{F} \quad MN/m^2 \tag{2.24}$$

2.5.3 Durability of cardan shaft forks

On the diagram of cardan shaft fork, force P is place on the fork at the center of U-bolt hole with a distance R.

Torsional stress $\tau = \dfrac{M_x}{W_x}$

Modulus of torsion of enlip cross section is defined as:

$$W_x \approx \frac{\pi h b^2}{16}$$

2.5.4 Power transmission performance of propeller shaft

At the frictional surfaces of the U-bolt, there will be wear and tear at the installation position of the needle bearings and also generating a high temperature upon unsecured lubrication. The cause of heat is due to the increased friction work

$$\eta = 1 - \frac{\mu d_1}{\pi r}\left[\ln tg(\frac{\pi}{4}+\frac{\alpha}{2})+tg\alpha\right] \tag{2.25}$$

We see that the performance of U-joint η depends on frictional coefficient μ and tilt angle α between the shafts. When α increases, performance η will decrease. When δ decreases, performance η will increase.

2.5.5 Heat at the U-joints

Due to the friction work on the U-bolt collar generating high temperature and heating U-joints. Solving the last equation and assuming that there is no temperature difference at the beginning T1 - T2 = 0 we will calculate the increase of temperature at the U-bolt collar as:

$$\tau = \frac{Q}{F''K}(1 - e^{\frac{t}{A_i}}) \tag{2.26}$$

8

With $A_1 = \dfrac{mc}{F''K}$; $\alpha = 4^o C$ (277°K) M$_o$=0,8M$_{emax}$; $\mu = 0,03$

2.6 Build finite element equation of propeller shaft assembly

Analyze the influence of dynamic parameters on the durability of propeller shaft, we use the finite element method (FINITE ELEMENT). The deformation and stresses within the element are represented by nodal displacement. The basic features of each element are:

The stiffness matrices of the elements are coupled into a stiffness matrix of the whole structure.

External forces cause internal force and displacement of the structure transformed to forces at the nodes and described in the equivalent nodal load matrix. The unknowns are nodal displacements (or internal forces at the nodes) defined in the nodal displacement matrix or nodal internal matrix.

Stiffness matrix, nodal displacement matrix, load matrix are in connection with each other in the linear balance equation.

In static case, the FINITE ELEMENT equation is formed as:

$$[K]\vec{u} = \vec{R} \qquad (2.27)$$

Where :

$[K]$ - Stiffness matrix

$\vec{u}$ - Vector of displacement results

$\vec{R}$ - Vector of forces

When vehicles operate, kinetic load is found in the structure, the FINITE ELEMENT equation is formed as:

$$[K][u] = [M].[\phi][\Omega^2] \qquad (2.28)$$

Where :

$[K]$: Stiffness matrix

$[M]$: Mass diagonal matrix

$[\Omega^2]$: Diagonal matrix of eigenvalues

$[\phi]$: Matrix of equivalent eigenvectors

Programming in ANSYS Workbench software, we receive the value of stiffness matrix parameters K, mass diagonal matrix M, diagonal matrix of eigenvalues Ω^2, matrix of eigenvectors ϕ. Displacement matrix u is the unknown to be found.

CONCLUSION OF CHAPTER 2

From the structure and operation principle of propeller shaft in light trucks, kinetic and dynamic models of universal joints and propeller shaft assembly in the power transmission system have been built as in reality.

Matlab Mupad and Simulink software application has developed a mathematical model with full equations defining kinetic relations and dynamic parameters of the system.

Identify the parameters which affect the durability of the propeller shaft to study 6 cases of propeller shaft with length of 1450mm, 1300mm, 1150mm and thickness of 6mm and 4mm.

Build finite element equation used as a basis to survey on the durability of the propeller shaft by kinetic and dynamic parameters and as the basis for applying FINITE ELEMENT software to simulate the survey.

Chapter 3
SURVEY ON THE INFLUENCES OF DYNAMIC PARAMETERS ON THE DURABILITY OF PROPELLER SHAFT

3.1 Assumptions

- Propeller shaft assembly lies in the vertical plane (passing through the focal point) and is the vertically symmetrical plane of the vehicle. The centerline of the propeller shaft coincides with the centerline of the power transmission system (POWERTRAIN)

- The centerline of the driving shaft and the driven shaft shall intersect with the centerline of the shaft body at the symmetrical center of universal joints.

- Ignore the deformation of each assembly in the vehicle, including the deformation of parts and the connection where the POWERTRAIN and the chassis of the vehicle have absolute stiffness.

- During the survey, ignore the interaction of oscillations between the assemblies in the POWERTRAIN and ignore the influence of the oscillations of automotive suspension system on the oscillation of the propeller shaft.

- Ignore the influence of the friction on the needle bearings at the rotating joints of the universal shaft and the spline tube on the body of the propeller shaft.

- The focal points of each part in the propeller shaft assembly are not shifted relatively during the motion of the system.

3.2 Survey on dynamics of propeller shaft assembly

3.2.1 Development of an algorithm diagram studying dynamics of propeller shaft assembly

Develop an algorithm diagram studying kinetics and dynamics of propeller shaft assembly by numerical method, Figure 3.1. After updating the parameters and defining the input variables including torque on the driving shaft τ, the tilt angle of the shaft in the vertical plane α, angular velocity ω, the calculating equation can be established.
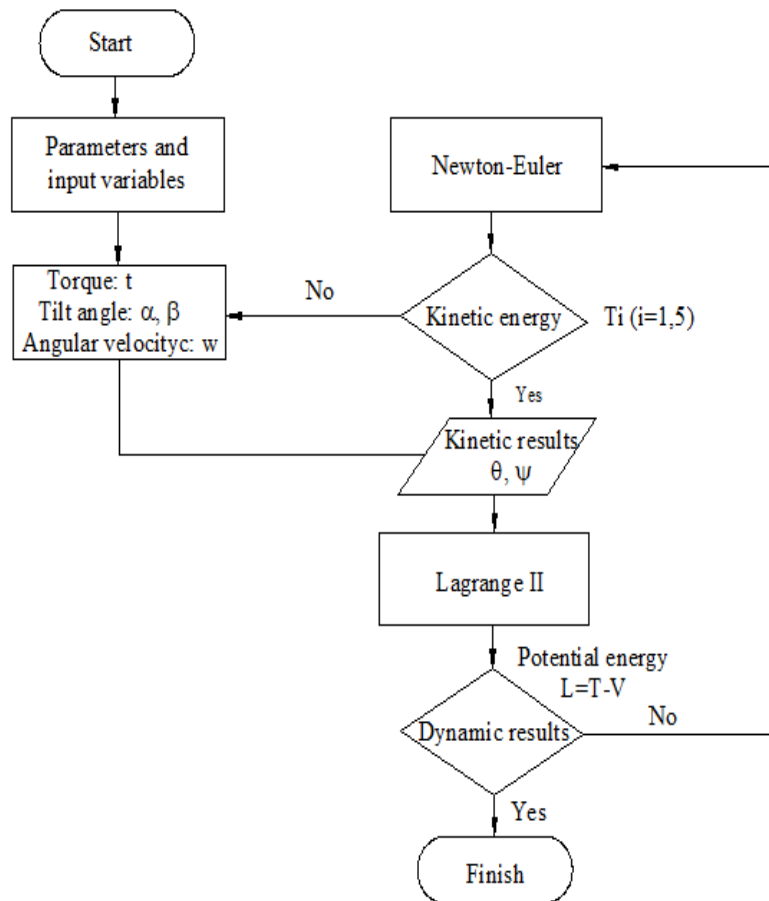
Figure 3.1 Algorithm diagram studying kinetics and dynamics of propeller shaft assembly

3.2.2 Development of Matlab Simulink diagram studying the dynamic parameters of the propeller shaft

Use the Matlab Simulink program to build a diagram for studying kinetics of propeller shaft. The results collected are the influence of the tilt angle in case $\alpha=0°,10°,20°,30°,40°$ and when the tilt angle of the shaft increases, the frequency of oscillation will increase respectively.
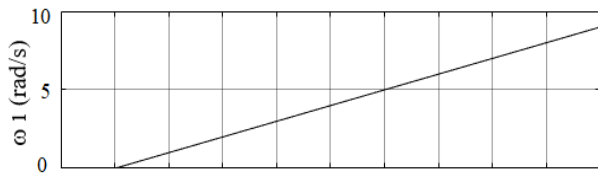
a) Velocity of input shaft
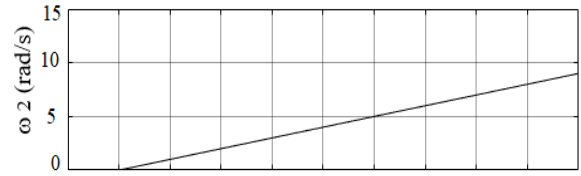
b) Velocity of middle shaft α = 0º
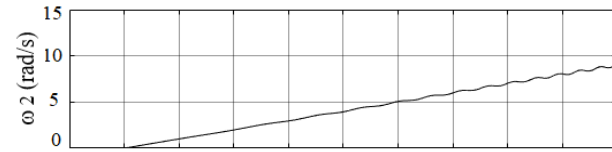
c) Velocity of middle shaft α = 10º
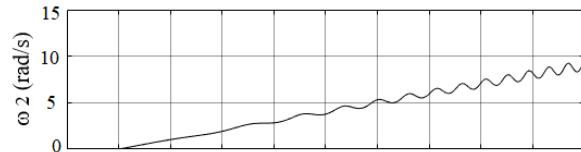
d) Velocity of middle shaft α = 20º
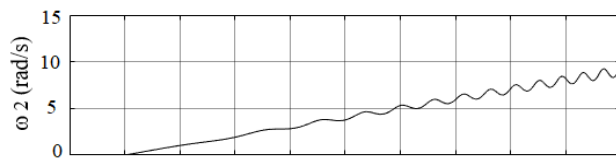
e) Velocity of middle shaft α = 30º
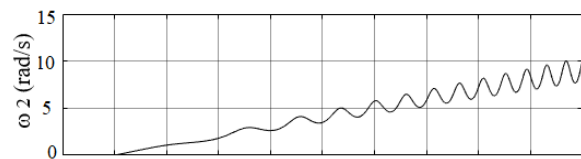
f) Velocity of middle shaft α = 40º

Figure 3.2 The results of the survey on the influence of tilt angle on the angular velocity of the propeller shaft

3.2.3 Angular motion of the U-bolt, input shaft, output shaft and angular momentum

The results of the survey on the angular displacement of the U-bolt omega, input shaft theta, output shaft gamma and angular momentum are shown in Figure. 3.3.
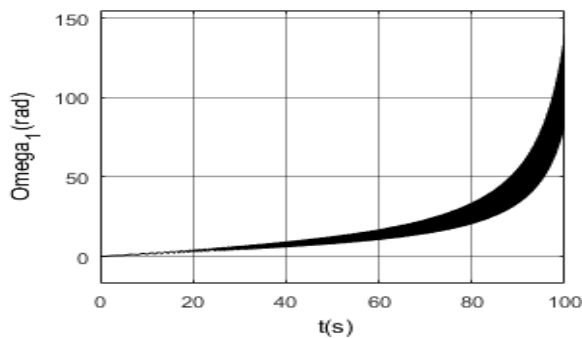
a) Omega angular displacement
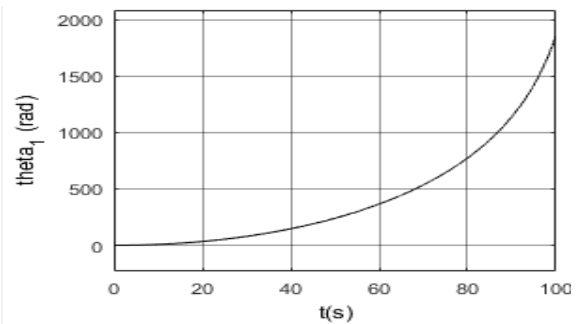
b) Theta angular displacement
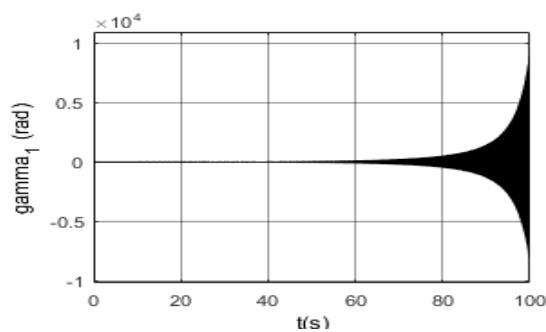
c) Gamma angular displacement
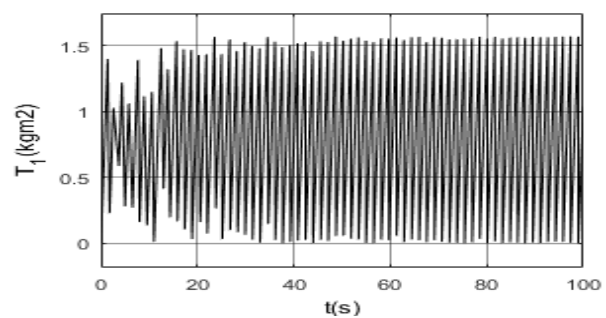
d) Angular momentum

Figure 3.3 Angular displacement and momentum of propeller shaft

3.3 Survey on the durability of propeller shaft

3.3.1 Development of an algorithm diagram studying the durability of propeller shaft

The algorithm used in calculating the durability of the propeller shaft in accordance with the FINITE ELEMENT method is built as in Figure 3.4.
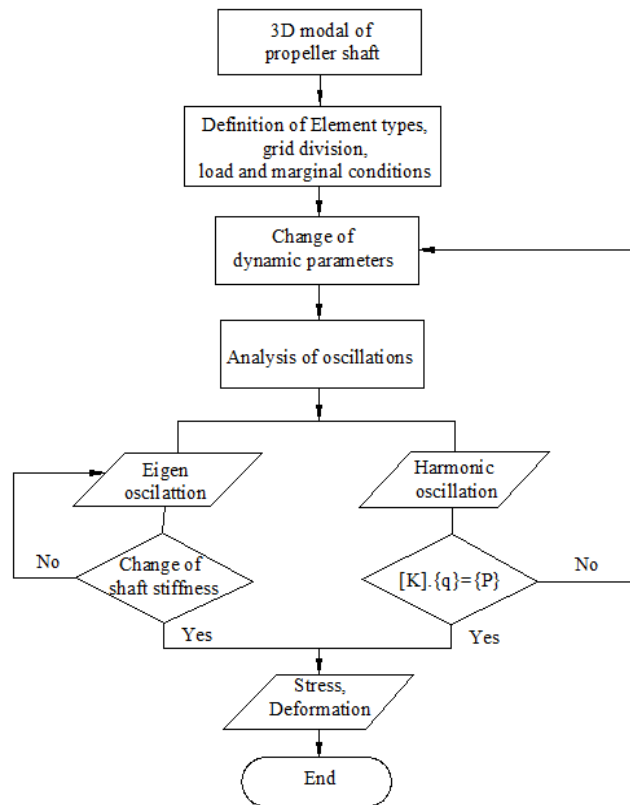
Hình 3.4 Algorithm diagram for calculating the durability of the propeller shaft

3.3.2 Development of material properties and composition of elements

From the analysis of propeller shaft structure, manufacturing materials and technology, we define the material properties of the propeller shaft with specific parameters based on the FINITE ELEMENT model.

3.3.3 Analysis of identification of element type

3.3.3.1 The number of elements

Establish an analysis table of the elements in the structure, we have the number of elements, the types of the elements and the analysis time. There are three types of 3D elements used in the math: SOLID187 (Quadratic Tetrahedral), CONTA174 (Contact) and TAGE170 (Contact).

3.3.3.2 The composition of elements

The elements used in the table are structured as including:

a) SOLID187; b) CONTA173; c) TARGE170

3.3.4 Analysis of eigen oscillations of propeller shaft assembly

3.3.4.1 Frequency range of eigen oscillations of the propeller shaft

In the FINITE ELEMENT equation (2.55), (2.56) We consider when force vector $R = 0$ to analyze eigen oscillations of the shaft, then we have the equation (3.1).

$$[M][\phi][\Omega^2] = 0 \tag{3.1}$$

Mass matrix $[M]$ is defined by the equation (2.58), Matrix of eigenvalues $[\Omega^2]$ is defined by the equation (2.59), matrix of eigenvectors $[\phi]$ is defined by the equation (2.60).

Apply Ansys Workbench software to programmatically analyze the eigen oscillation of the shaft, at 20 types of oscillations corresponding to the eigen frequency range.
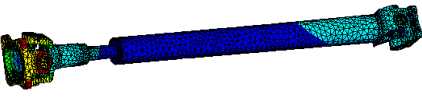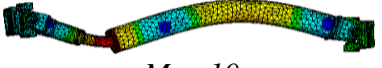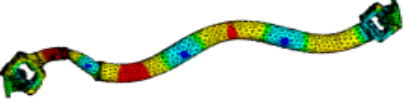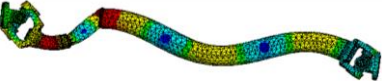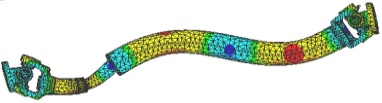
3.3.4.2 Bending oscillation

Use L as the length of the shaft; M is the number of eigen types; f as frequency of oscillation; Df as maximum displacement.

a) The influence of the length of the propeller shaft on bending oscillation

The length of propeller shaft does not affect bending oscillation, because the stiffness of the propeller shaft assembly is within the allowable limit of the structure. The survey results are shown in Table 3.1.
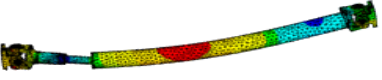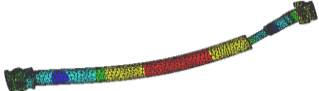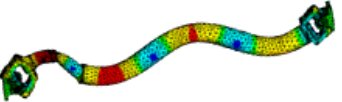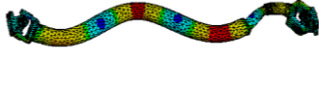
Table 3.1 The influence of the shaft length on the bending oscillation of the propeller shaft

L 1450x6 mm	L 1300x6 mm	L 1150x6 mm
M = 10 f = 654.69 Hz Df = 0.71621 m	M = 10 f = 667.68 Hz Df = 0.72923 m	M = 10 f = 543.93 Hz Df = 0.38202 m
M = 15 f = 1295.9 Hz Df = 0.29754 m	M = 15 f = 1451.6 Hz Df = 0.33596 m	M = 15 f = 1157.9 Hz Df = 0.3481 m

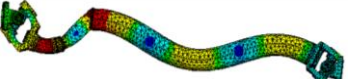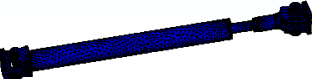**b) The influence of the thickness of the propeller shaft on bending oscillation**

At the frequency below 600 Hz, the shaft is bended; the average frequency from over 600 Hz to below 1000 Hz, the shaft is more twisted and at the frequency over 1000 Hz, the shaft is bended and twisted, in which torsional displacement is at a very large amplitude.

Table 3.2 The influence of the thickness of the propeller shaft on bending oscillation in case of L1450mm

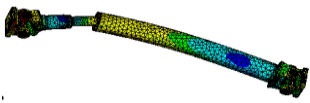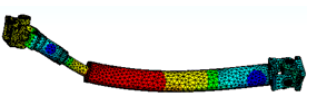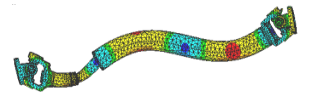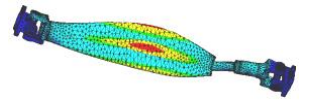| L 1450x6 mm		L 1450x4 mm	
	M = 6 f = 185.0 Hz Df = 0.29532 m		M = 6 f = 186.43 Hz Df = 0.34239 m
	M = 15 f = 1295.9 Hz Df = 0.29754 m		M = 15 f = 1312.9 Hz Df = 0.35496 m

On the L1300 mm shaft, the survey results show that similar to the L1450 mm shaft, at the frequency below 600 Hz, shaft is more flexed and small parts on the two ends of the shaft such as the universal bearing snap rings and gaskets will be more affected

Table 3.3 The influence of the thickness of the propeller shaft on bending oscillation in case of L1300mm

L 1300x6mm		L 1300x4mm	
	M = 6 f = 204.42 Hz Df = 0.31992 m		M = 6 f = 209.54 Hz Df = 0.35938 m
	M = 15 f = 1451.6 Hz Df = 0.33596 m		M = 15 f = 1081 Hz Df = 71.347 m (Vòng chặn bi)

On shorter shaft of L1150 mm, the survey results show that in the frequency range below 600 Hz, the shaft is almost flexed; The average frequency range above 600 Hz to below 1000 Hz, the shaft is bended and twisted and at the frequency above 1000 Hz, the shaft is at maximum twist, in which the torsional displacement is at a very large amplitude and oscillation type is also more diversified.

13
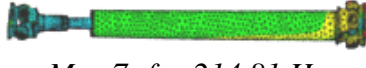
L 1150x6mm		L 1150x4mm	
	M = 6 f = 230.16 Hz Df = 0.35885 m		M = 6 f = 233.89 Hz Df = 0.37169 m
	M = 15 f = 1157.9 Hz Df = 0.3481 m		M = 15 f = 1617 Hz Df = 0.73519 m

3.3.4.3 Torsional oscillation of propeller shaft
a) Influence of shaft length on bending oscillation of the propeller shaft

The survey shows that the shaft length has a great influence on torsional oscillation of the propeller shaft because of the influence of the stiffness of the assembly. The survey results are shown in Table 3.5.

Table 3.5 Influence of shaft length on torsional oscillation of the propeller shaft

L 1450x6mm	L 1300x6mm	L 1150x6mm
 M = 7; f = 214.81 Hz Df = 0.42168 m	 M = 7; f = 226.12 Hz Df = 0.44134 m	 M = 7; f = 238.46 Hz Df = 0.46369 m
 M = 20; f = 1081.9 Hz Df = 0.63633 m	There is no torsional oscillation	There is no torsional oscillation

b) Influence of shaft thickness on torsional oscillation of the propeller shaft

The shaft thickness has a great influence on the torsional oscillation. The survey results are shown in Tables 3.6, 3.7 and 3.8. Of the same length, the shaft has different thickness, the oscillation of the shaft also varies. Shaft with thickness of 4 mm will have larger torsional displacement than the 6 mm shaft in thickness.

Table 3.6 Influence of shaft thickness on torsional oscillation of the propeller shaft in case of L1450mm

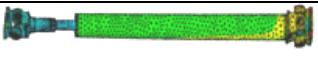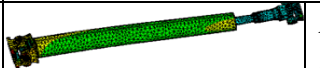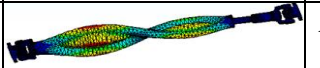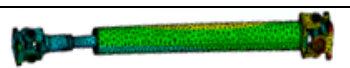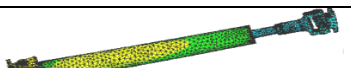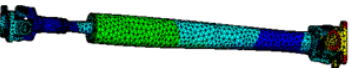| L 1450x6mm		L 1450x4mm	
	M = 7 f = 214.81 Hz Df = 0.42168 m		M = 7; f = 255.76 Hz Df = 0.43999 m
	M = 20; f = 1081.9 Hz Df = 0.63633 m		M = 19; f = 1669.4 Hz Df = 0.65885 m
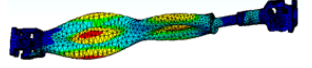
On the L1300 mm long shaft, the survey results show that at the frequency below 600 Hz, the shaft is almost more twisted than at the average and high frequency. The survey results on the L1300 mm shaft are shown in Table 3.7. The torsional oscillations occur at all three low, medium, and high frequency for shafts with thickness of 6 mm. For shafts with thickness of 4 mm, torsional oscillations occur at low and high frequency.

Table 3.7 Influence of shaft thickness on torsional oscillation of the propeller shaft in case of L1300mm

L 1300x6 mm		L 1300x4 mm	
	M = 7 f = 226.12 Hz Df = 0.44134 m		M = 7 f = 226.12 Hz Df = 0.44134 m
	M = 14 f = 1175.4 Hz Df = 0.61395 m	There is no torsional oscillation	

For the L1150 mm shaft, the survey results show that the torsional oscillation occurs in shafts with smaller thickness and the oscillation occurs at all low, medium and high frequency regions. The survey results of the L1150 mm shaft are presented in Table 3.8.

Table 3.8 Influence of shaft thickness on torsional oscillation of the propeller shaft in case of L 1150mm

L 1150x6mm		L 1150x4mm	
	M = 7; f = 238.46 Hz Df = 0.46369 m		M = 7; f = 260.59 Hz Df = 0.48496 m
There is no torsional oscillation			M = 20; f = 1731.2 Hz Df = 0.74466 m

3.3.5 Analysis of harmonic motion distributed on propeller shaft

When stimulation force *R* works, the shaft is in torsional oscillation during operation.

3.3.5.1 Input parameters

Stimulation force is the torque on the shaft transmitted from the engine through the clutch and the gearbox. The maximum torque value of the engine is defined by nominal value Me_{max} = 320Nm at 2200 rpm. Drag torque from driving wheel is M_k = 225Nm.

3.3.5.2 Parameters of Marginal conditions

We select constraints in the FINITE ELEMENT structure satisfying the marginal conditions in the simulation model which are the two positions A_1 and B_1 on the two shaft ends placed on object 5.

The marginal condition parameters are identified to ensure enough stiffness for the whole shaft on the structure and stability during mechanical work and satisfy the assumptions given in 3.1.
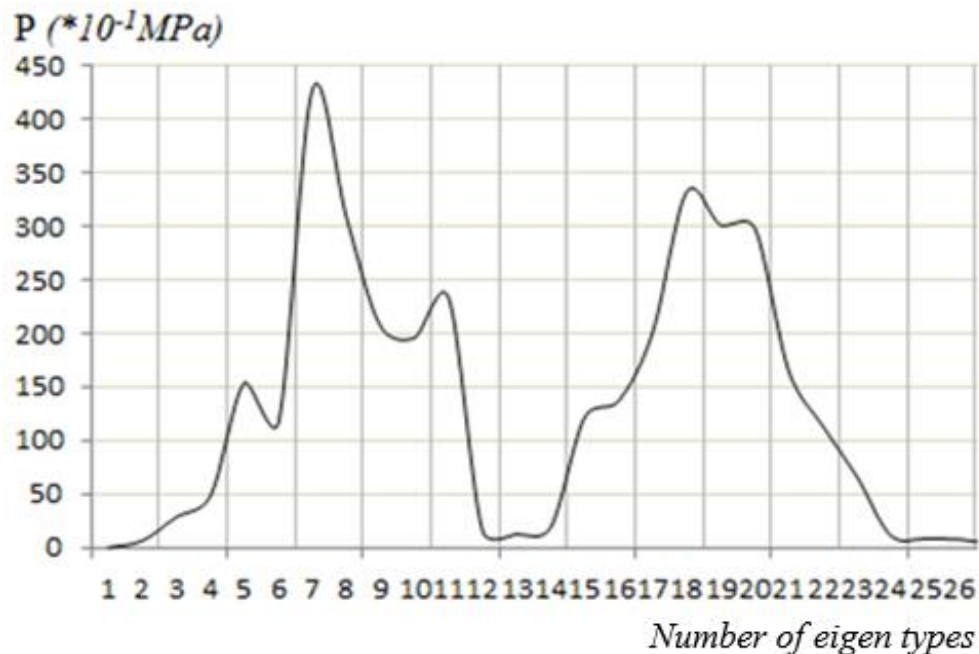
Figure 3.5 Graph of load distribution by frequency L 1450 x 6 mm

7th eigen type, f = 508.22Hz, P = 42.8116 Mpa

18th eigen type, f = 2122.975Hz, P = 33.2166 MPa

3.3.6 Distribution of stress and deformation on propeller shaft

3.3.6.1 On propeller shaft assembly

Using Ansys Workbench finite element software, we receive stress and deformation values on the propeller shaft assembly. The advantage of software usage is that full marginal conditions can be inserted into the math. The results are directly reflected in the 3D graph of the details which can be read easily through color spectrum and display values.

15

a) Distribution of bending stress

b) Distribution of torsional stress

c) Distribution of deformation on propeller shaft fork

d) Distribution of deformation on flange

Figure 3.6 Distribution of stress and deformation on propeller shaft

3.3.6.2 On the body of the shaft

On the shaft body, one end is attached to the fork, the other end is attached to the spline shaft, a hollow round tube in the middle of which two ends are welded tightly into a solid block. The geometric properties of the solid block include:

Volume: $517.83mm^3$; Weight: 4.065 kg; Focal coordinates: x, y, z = -158.71, -129.03, 275.64 mm; Number of nodes: 7384; Number of elements: 4034.

Simulation results show that maximum deformation is 2.453 mm/mm ; maximum stress is 262 Mpa. The simulation results by images are shown in Figure 3.7.

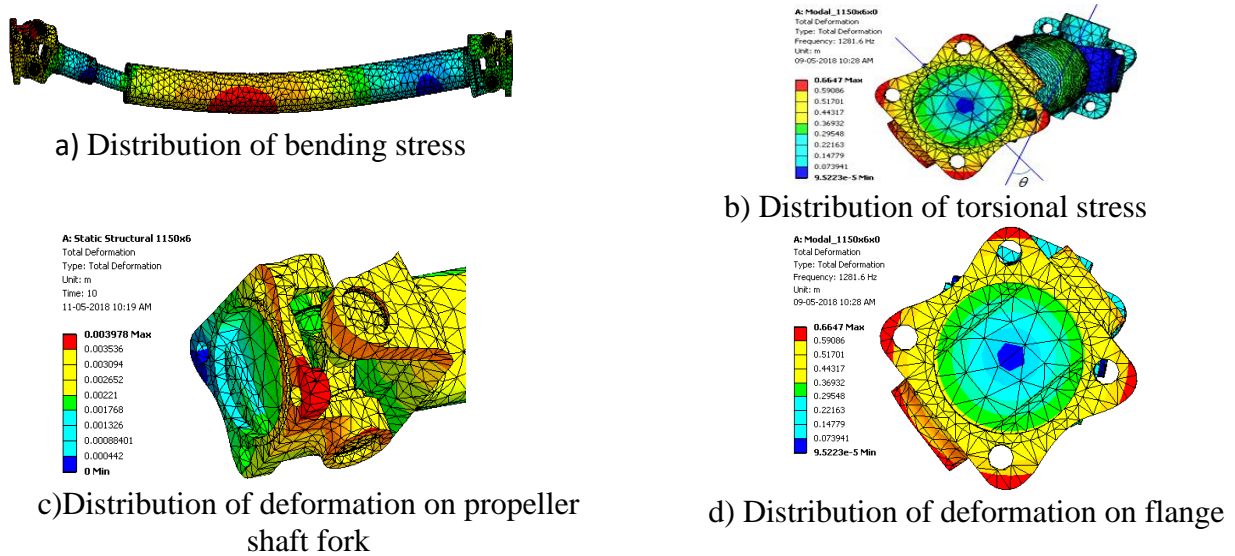*Figure 3.7 Simulation results of the durability of propeller shaft*

3.3.6.3 On the shaft fork

Similar to the simulation of the shaft body, we implement the same simulation with the shaft fork and receive results as follows:
Volume: $398.7mm^3$; Weight: 3.13 kg; Focal coordinates: x, y, z = 4.278, 11.65, 19.318 mm; Number of nodes: 13794; Number of elements: 7172.

Simulation results show that maximum deformation is 3.788 mm/mm; maximum stress is 399 Mpa. The simulation results by images are shown in Figure 3.8.

Figure 3.8 Simulation results of the durability of cardan shaft fork

3.3.6.4 On the U-bolts

Implement the same simulation as done with the shaft body and fork, we receive the simulation results of the U-bolt:

Volume: $104.6mm^3$; Weight: 0.821 kg; Focal coordinates: x, y, z = 1.136, 3.215, 0.877 mm; Number of nodes: 33583; Number of elements: 19753.

Simulation results show that maximum deformation is 0.476 mm/mm; maximum stress is 265.3 Mpa. The simulation results by images are shown in Figure 3.9.
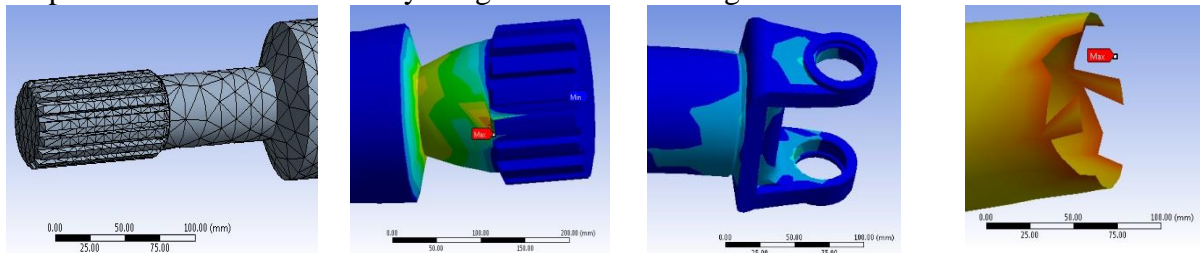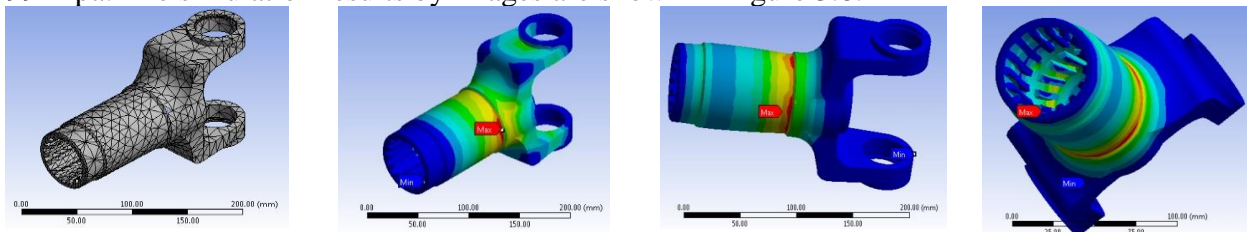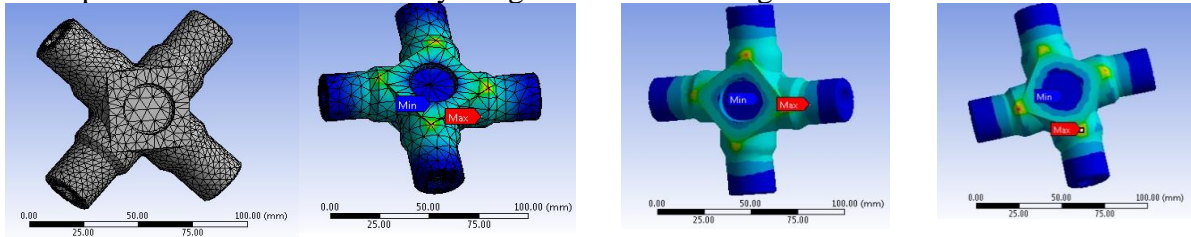

Figure 3.9 Simulation results of the durability of the universal shaft

3.3.7 The influences of geometric parameters on stress and deformation

3.3.7.1 Influence of length on stress and deformation on the shaft

Result comparison in terms of length shows that shaft 1 with L1450x6mm will have larger total displacement of equivalent deformation and stress than shaft 2 and 3 with shorter length.

On the longer shaft with L1450x6mm, the equivalent deformation is 3.8589e-002 m / m and the equivalent stress is 7.7178e + 009 Pa which is the largest compared to the two shorter shafts.

Medium-length shaft with L1300x6mm has the largest total displacement. Consequently, shaft 1 is less durable than the shaft 2 and 3.

Survey results are shown in Table 3.14.

Table 3.14 Influence of length on stress and deformation on the shaft

	L1450x6mm	L1300x6mm	L1150x6mm
Total displacement (m)	5.4589e-003	**5.6786e-003**	3.978e-003
Relative displacement (m/m)	**3.8589e-002**	3.2706e-002	3.7625e-002
Relative stress (von-Mises) (Pa)	**7.7178e+009**	6.2989e+009	7.5251e+009

3.3.7.2 Influence of thickness on stress and deformation on the shaft

Thickness has the greatest impact on stress and deformation of propeller shaft during operation. From the results of this survey, we can identify the number of nodes, the number of elements of each type of shafts. With different thickness, the number of nodes and the number of elements per shaft are also different.

Result comparison in term of thickness shows that the 4 mm thin shaft will have greater parameters of equivalent deformation and stress than the 6 mm shaft. This case also shows that thinner shaft of 4 mm is less durable than the 6 mm shaft.

Survey results are shown in Table 3.15.

Table 3.15 Influence of thickness on stress and deformation on the shaft

	Shaft 1		Shaft 2		Shaft 3	
	1450 x 6	1450 x 4	1300 x 6	1300 x 4	1150 x 6	1150 x 4
Number of nodes	428680	427772	424571	424429	420636	420176
Number of elements	243230	242214	241281	240611	239245	238549
Total displacement (m)	5.4589e-003	**6.6223e-003**	**5.6786e-003**	3.5592e-003	3.978e-003	**5.2456e-003**
Relative displacement (m/m)	3.8589e-002	**4.7135e-002**	3.2706e-002	**3.5592e-003**	3.7625e-002	**5.6015e-002**
Relative stress (von-Mises) (Pa)	7.7178e+009	**8.8614e+009**	6.2989e+009	**8.1948e+009**	7.5251e+009	**1.1152e+010**

3.3.7 Influence of dynamic parameters on the durability of propeller shaft

The survey on the influences of dynamic parameters on the propeller shaft includes stiffness depending on length, thickness and oscillation frequency, eigen oscillation types affecting the durability of the propeller shaft. ANSYS Workbench software application provides the analysis results shown in Figure 3.10 for shaft with length L = 1450x6mm and Figure 3.11 for shaft with length L = 1300x6mm. The purpose of the survey on the two types of shafts is to compare with the two shaft used in the experiment of the same type.
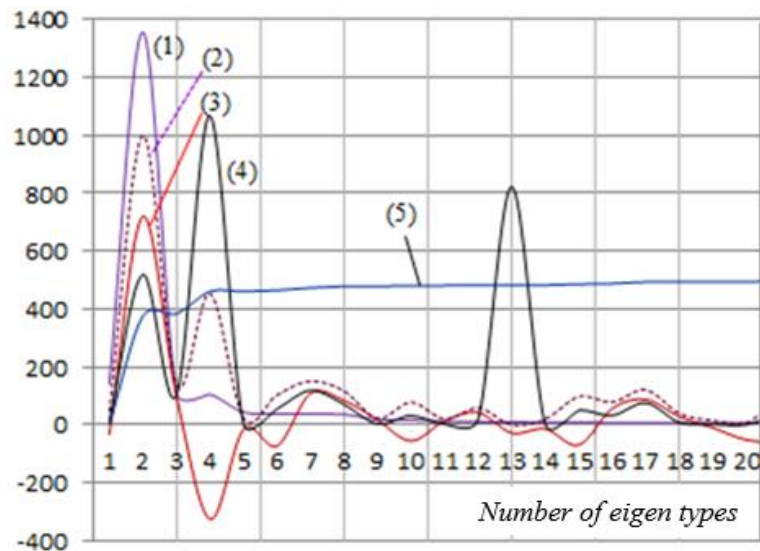
—————— 1) Deformation to direction X (*10^{-3}mm), ε_x= 1357.1 at 374.73Hz
- - - - - - 2) Deformation to direction Y (*10^{-3}mm), ε_y= 453.794 at 374.73Hz
—————— 3) Deformation to direction Z (*10^{-3}mm), ε_z= 719.96 at 374.73Hz
—————— 4) Total displacement (mm/m) Df = 518.435 at 1295.9Hz
—————— 5) Total torsion angle (rad) θ = 500 at1801.9Hz

Figure 3.10 Graph of deformation,displacement, total torsion angle on shaft L=1450 x6mm
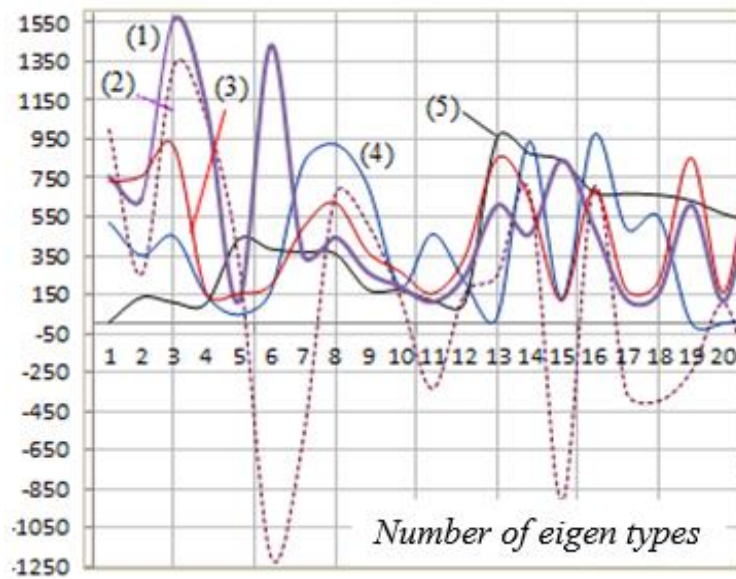
—————— 1) Deformation to direction X (*10^{-3}mm), ε_x= 1566.75 at 441.6 Hz
- - - - - - 2) Deformation to direction Y (*10^{-3}mm, ε_y =1326.61 at 441.6Hz
—————— 3) Deformation to direction Z (*10^{-3}mm), ε_z= 914.153 at441.6Hz
—————— 4) Total displacement (mm/m) Df = 875.35 at 1451.6 Hz
—————— 5) Total torsion angle (rad) θ = 973.6 at 2007.8 Hz

Figure 3.11 Graph of deformation,displacement, total torsion angle on shaft L=1300x6mm

Based on the above graphs, we can establish a table of result analysis as in table 3.16 which clearly shows that directional deformation, total displacement and torsion angle on the shaft with L = 1450mm is larger than on the L = 1300mm long shaft. This result will be verified in the experiment.

18

Table 3.16 Survey result of deformation, total displacement, and torsion angle on the propeller shaft

Shaft length x 6mm	Eigen type	Frequency (Hz)	Deformation to direction x ($*10^{-3}$mm)	Deformation to direction y ($*10^{-3}$mm)	Deformation to direction z ($*10^{-3}$mm)	Total displacement (mm/m)	Total torsion angle of the shaft (rad)
L = 1450	9	374.73	1566.75	1326.61	914.153	-	-
L = 1450	15	1295.9	-	-	-	875.35	-
L = 1450	20	1801.9	-	-	-	-	973.6
L = 1300	9	441.6	1357.1	-	719.96	518.435	-
L = 1300	15	1451.6	-	453.794	-	-	-
L = 1300	20	2007.8	-	-	-	-	500

CONCLUSION OF CHAPTER 3

The development of an algorithm studying the kinetics and dynamics of propeller shaft shows the influences of geometric parameters such as tilt angle, length and anti-torsional stiffness (related to the thickness of the shaft) on kinetics, dynamics of the propeller shaft. Application of Matlab Mupad and Simulink software simulates the kinetic survey of the asemblies, defines the relationship between the speed of input shaft, output shaft, middle shaft and the influence of tilt angle in cases of $\alpha = 0^0$, 10^0, 20^0, 30^0, 40^0 to identify the oscillation frequency of the main shaft when the number of rotations increase.

Develop an algorithm to calculate the durability of the propeller shaft and determine the finite element method for the simulation. Use the specialized Ansys Workbench software to solve the math. The simulation results are accurate because of the appropriate identified element types.

Identify eigen oscillation types of the propeller shaft assembly in the following six cases: (1) L1450 x 6mm, (2) L1450 x 4mm, (3) L1300 x 6mm, (4) L1300 x 4mm, (5) L1150 x 6mm, (6) L1150 x 4mm. The results show the bending and torsion oscillations in each case as the data basis for the design of propeller shaft.

Define the frequency of harmonic oscillations of the force as the basis for the survey on the durability of the assembly and the components on the shaft depending on kinetic, dynamic parameters of the durability of the shaft, the results are obtained in the reliable form of numerical table, 2D graph and 3D model.

Chapter 4
EXPERIMENTAL RESEARCH

4.1 Experimental purposes

The purpose of this test is to define the relationship between dynamic parameters and the durability of propeller shaft through the measured results including the value of torque and deformation on the shaft when the shaft is rotating in the load modes corresponding to the working mode of the real vehicle.

4.2 Experimental object

Experimental object is an assembly of propeller shaft in the power transmission system of light trucks with load of up to 3 tons LF 3070G1 type produced and assembled in Vietnam.

4.3 Parameters in the experiment

Experimental parameters are describes in Figure 4.1 including:

Predefined parameters include: Number of rotations n (v/ph); Length of the shaft L_{cd} (mm); Tilt angle α (degree).

Measurable parameters in the experiment include: torque on the shaft M_{cd} (Nm); stress to the direction X at measured position σ_x (N/m^2); deformation to direction X on the shaft surface at the measured position ε_x (mm).
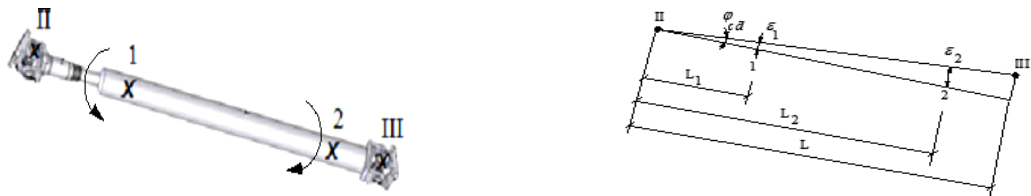
a) Measurement positions no. 1 and 2   *b) Geometry of 2 measurement points.*

Figure 4.1 Simulation model of experimental parameters on propeller shaft

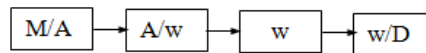## 4.4 Development of experimental diagram

Figure 4.2 shows an experimental diagram measuring the parameters when shaft 1 is rotating by driving torque M_e, load torque M_c in correspondence with working state of the actual vehicle..

Received signals are mechanical quantities such as torque, deformation, number of rotations (non-electrical quantity) converted into voltage Δ_e by sensor tenzo pasted on the shaft 1 at the two measured positions. Using a converter circuit to convert voltage Δ_e into electromagnetic wave w transmitted into the space. Also use the converter circuit to convert the electromagnetic wave into the voltage to collect for the next circuit which is the digital signals brought into computers with processing software to obtain the initial results such as moment, deformation, and number of rotations. The device with these converter circuits is called the wireless transceiver No. 2 and 3 in Figure 4.2a.

The wireless transceiver No.3 is installed into the computer No. 4 through the COM port. Voltage signal Δe received from tenzo has a low voltage <10mV transmitted to the computer, and after being amplified, converted to A/D (Analog/Digital) for the micro-controller to perform the processing, display the measurement and record the measured results into a file stored in the computer, Figure 4.2b.
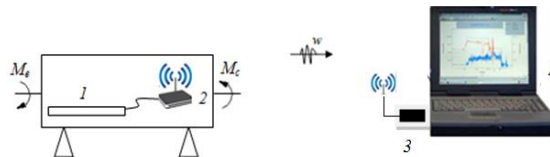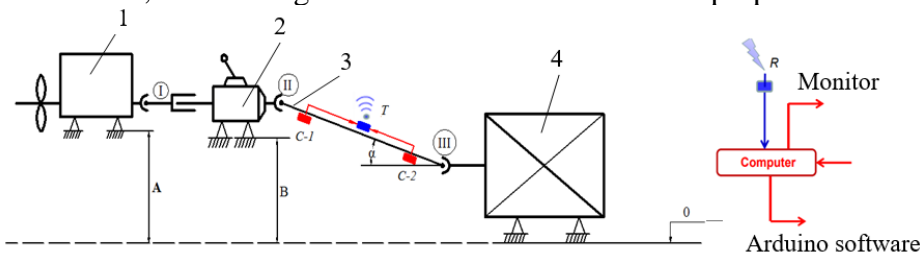

a) Diagram of experimental devices

b) Diagram of signal transmission

Figure 4.2 Experimental diagram

1. Propeller shaft, 2. Signal transmitter, 3. Signal receiver, 4. Computer, w.Signal transmitted wave

4.5 Design of experimental platform for propeller shaft

The experiment has designed an experimental platform according to the principle of open power current shown in diagram 4.3 including IVECO 81kW diesel-type driving engine, five-gear manual transmission and propeller shaft tiltly installed in the vertical plane of which angle can be changed with the value α corresponding to the assemblies installed in the real vehicle, MP100S load generation structure, wireless signal transmitter mounted on the propeller shaft.

1. IVECO 81kW diesel-type driving engine, 2. Five-gear manual transmission, 3. Propeller shaft, 4. MP100S load generation structure

Figure 4.3 Diagram of experimental platform for propeller shaft

Experimental cases include changes of tilt angle, length and the number of rotations at load modes corresponding to the load mode of an actual vehicle when it operates on the road. At C-1,

C-2 positions, tenzo is pasted on Whenzone bridge to obtain signals to transmit to the transceiver and wireless receivers T and R and converted to torque and deformation signals by standard gauge measured on special machines.

Use the FCA-3-11 defomation Tenzo (Fig. 4.4) manufactured by Tokyo Sokki Kenkyjo of Japan with the following basic parameters: length 3 mm, resistance 120±0.5 Ω.

Figure 4.4 Deformation Tenzo used in experimental research

On the torque-measured shaft, paste tenzo directly onto the cleaned polished surface by using a special glue, connect the sensor wires into a bridge and take the wires out. Proceed to paste tenzo on the shaft at the two ends of the shaft. The Wheatstone Bridge (consisting of four resistors: R1, R2, R3 and R4) is used as a measurement circuit for tenzo resistor. The two ends of the bridge are connected to the power supply, the other two ends are connected to the measuring device, Figure 4.5.
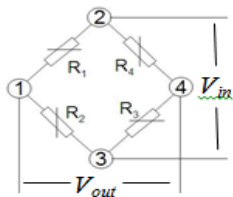

Figure 4.5 Circuit of Wheatstone bridge and tenzo pasted on the shaft

With tenzo made of metal material, the voltage V_{out} is almost proportional to the deformation of the shaft, which is proportional to the torque on the shaft M_t, therefore the measurer can be considered as linear.

$$V_{out} \approx k.M_t \tag{4.1}$$

Where k is the scaling factor, Mt is the torque on the shaft.

Computer and Software Programming:Use desktop computer or notebook installed with programming software C # and display interface design in Visual Studio. The measured signals are recorded, displayed on the screen and saved to a file on the computer.

Design and manufacture wireless signal transceiver with overall design plan and manufacturing results achieved:

1. *Generating circuit;* 2. *Receiving circuit;*
3. *Battery (type 3,3V)*

Figure 4.6.Overall design plan of wireless transceiving circuit measuring velocity and deformation

Figure 4.7. Images of wireless transceiver designed and manufactured.

Overall diagram of experimental platform after installation and calibration presented in Figure 4.8
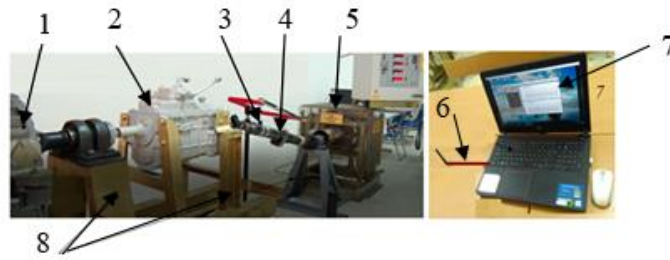
1. Driving engine; 2.Gearbox; 3.Propeller shaft; 4. Transmitter; 5. MP100S load generator;
6. Receiver; 7. Computer; 8. Carrier
Figure 4.8 Experimental platform for propeller shaft

4.6 Calibration of measurement signal

- Calibration of measurement deformation is performed on a specialized machine with wireless transceiver to transmit and receive signals.

Calibration of torque on the propeller shaft is in accordance with Formula (4.2).

$$M_{xcl} = P_t.l_{cl} \tag{4.2}$$

Measuring voltage Δe (mV) and torque M_{xcl} (Nm) is linear, nearly based on Formula (4.3).

$$\Delta e \approx k_M.M_{xcl} \tag{4.3}$$

Where: k_M is the scaling factor, M_{xcl} is the caliper torque on the shaft.

The results identify the value of caliper torque as 25kgm/10mV

Calibrate torque on the MP100S load generating device with standard gauge weight of 25kg, arm length of 1000mm, torque of 250 Nm as well as calibration of wireless transceiver.

Comparison of the results shows that the difference between the two transceivers is 0.3%, therefore the wireless transceiver is reliable.

4.7 Experimental modes

Experimental modes are tested in Table 4.1 with 2 shafts of different length L_1=1300mm *and* L_2 = 1450mm; 2 tilt angles: α = 10º and α = 15º; 2 load modes: on MP100S load generating device including load 1 = 100N.m and load 2 = 200N.m (equivalent to 50% load and 100% load of the vehicle).

Results of calibration identify the value of standard gauge deformation of resistance *ε (μm)* 0.1550mm/10mV.

Table 4.1 Experimental modes

4 inputs	1. Load mode (N.m)	100	200
	2. Number of rotations n_t (v/ph)	1000	2000
	3. Shaft length L_t (mm): 1300/1450		
	4. Tilt angle of the shaft: $α_1=0^O$, $α_2=15^O$		
	Measured position of deformation 1/2	*Symbol of measurement file at position 1, end I*	*Symbol of measurement file at position 2, end II*
2 outputs Simultaneously measured	(I) $ε_{11}$, $ε_{21}$ (μ_m)	BD -11.01	BD -21.02
	(I) $ε_{12}$, $ε_{22}$ (μ_m)	BD -12.01	BD -22.02
	(I) $ε_{13}$, $ε_{23}$ (μ_m)	BD -13.01	BD -23.02
	(II) n_{11}, n_{21} (v/ph)	n11.01	n21.02
	(II) n_{12}, n_{22} (v/ph)	n12.01	n22.02
	(II) n_{13}, n_{23} (v/ph)	n13.01	n23.02

Used symbols for the saved file of the results: The word "BD" refers to deformation; The "n" refers to angular velocity; The first number "1, 2" is the measurement position 1, 2 or I, II; The second number "1, 2, 3" represents the measurement turns; Indicator "0" is angle of inclination of the shaft; Indicator "1" is load mode.

4.8 Steps of experimental performance on the platform

Experimental steps are carried out in the following orders: Installing propeller shaft glued with tenzo, installing the wireless transceiver into the computer, calibrating moment of load generator, implementing experiment on the platform. Experiment results are displayed the interface as shown in the figure.

Implement three times for each measurement to get the average value. Then the number of experimental turns for each shaft are: 2 load modes (100N.m and 200N.m) x 2 modes of number of rotations (1000 v / ph and 2000 v / ph) x 2 modes of tilt angle (0o and 15o) x 3 turns = 24 experiments equivalent to 24 results saved. The experiments on 2 shafts with L1350mm and L1400mm have 48 results saved in the computer.

4.9 Some results obtained after experiments

The results in Figure 4.9 show the influence of length on deformation on the shaft. When rotating with the same number of rotations and the same load mode, deformation at position 2 on the 1450 mm long shaft is larger than the deformation on the 1300 mm short shaft. Herein we calculate the torsion angle as:

On short shaft L = 1300mm:

$$tg\varphi_{cd} \approx \varphi_{cd} = \frac{1.8}{900} = 0.002 \quad (rad)$$

On long shaft L = 1450mm:

$$tg\varphi_{cd} \approx \varphi_{cd} = \frac{2.15}{900} = 0.0024 \quad (rad)$$

The tilt angle and length of the shaft have great impact on the deformation of the 2 shaft ends. The results of measuring two deformation values at the two ends can be seen clearly in Figure 4.10. From the measurement results, we can calculate the deformation on the short and long shafts as:

On short shaft L = 1300mm:

$$tg\varphi_{cd} \approx \varphi_{cd} = \frac{1.593}{900} = 0.00177 \quad (rad)$$

On long shaft L = 1450mm:

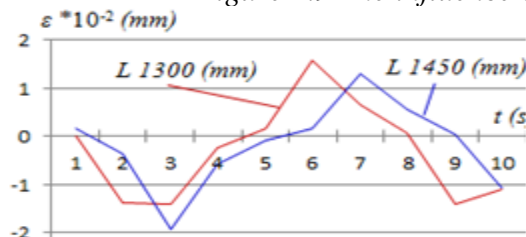$$tg\varphi_{cd} \approx \varphi_{cd} = \frac{3.522}{900} = 0.0039 \quad (rad)$$
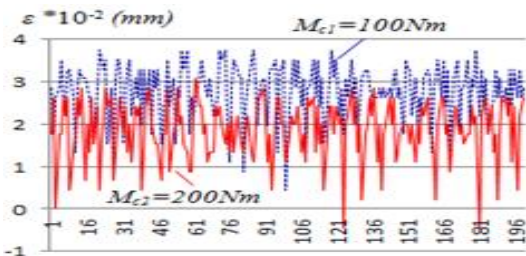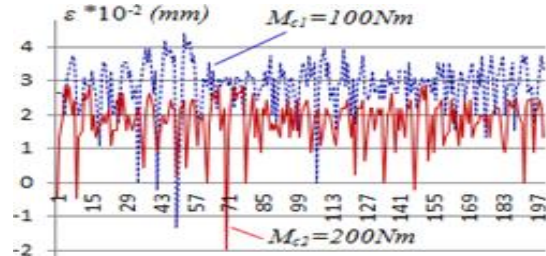
a) On shaft with length L = 1300mm   *b) On shaft with length L = 1450mm*
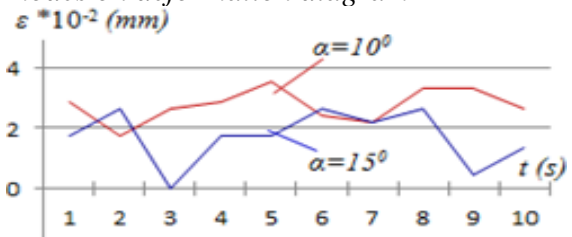
Figure 4.9 The influence of load modes on deformation diagram

a) On shaft with length L = 1300mm   *b) On shaft with length L = 1450mm*

Figure 4.10 The influence of length and tilt angle of propeller shaft on deformation

At the same measuring distance L2 = 900mm, due to the difference in the length of load torque placed on two shafts, the deformation of the two shafts are also different leading to the difference in the angles of relative torsion on the two shafts which is consistent with the torsion theory on the shaft in static state.

CONCLUSION OF CHAPTER 4

Use tenzo sensor based on the principle of Wheatstone bridge on two shaft ends of the powertrain in trucks with load of up to 3 tons. Design and manufacture experimental platform for the open power current satisfying the experimental requirements of the thesis.

Design and manufacture wireless transceivers ensuring the experimental requirements with economic efficiency, effectiveness and reliability.

Simultaneously measure torque, stress, and number of rotations on the rotating shaft with different load modes according to Wheatston bridge circuit principle. The output signals using the principle of wireless electromagnetic wave transceiver transmitted to the processing amplifier allow to remain the actual state of the assemblies and the generated load modes are in accordance with the load mode of a vehicle when it operates on the road, therefore the results are reliable.

Experiment results show that the 1450 mm long shaft has larger deformation than the 1300 mm shaft and hence the stiffness condition of the shorter shaft is more satisfactory than the long shaft. It is particularly true when the distance is too far, we need to use the dual shaft to transmit power in the vehicle's powertrain. The measurement results are productive and reliable.

Based on this, it is possible to measure torque simultaneously on the three shafts of other mechanical assemblies and evaluate the quality of the axles for the development of automobile localization in practice.

CONCLUSION OF THE THESIS AND FURTHER RESEARCH DIRECTION

Conclusion

1. Develop a spatial model of propeller shaft in the power transmission system of trucks with load of up to 3 tons by kinetics and dynamics of multi-body system reflecting the actual working status of propeller shaft in the vehicle;

2. Define the Lagrange-Dalember method to write the equation describing the motion of propeller shaft; solve the differential equation of motion and simulate the survey on the kinetics of assemblies by Matlab Mupad and Simulink;

3. Use finite element method with ANSYS Workbench software, a new scientific tool to simulate the survey on the durability of propeller shaft;

4. Design and manufacture experimental platform for the open power current with modern equipment and reliable results;

5. Design and manufacture wireless signal transceiver using the wiless principle to obtain signals on the rotating shaft; values are deformed from the transfer of non-electrical signal to electrical signal and digital signal in the experiment and standard gauge measured on the same wireless transceiver..

6. Compare the simulation results and experimental results:

Shaft length (mm)	Deformation (*10⁻³mm)			Total torsion angle of the shaft (rad)		
	Calculation	experiment	Difference (%)	Calculation	experiment	Difference (%)
L = 1300	1357.1	1800	13	0.0015	0.0017	12
L = 1450	1566.75	2150	17	0.0031	0.0039	21

The comparison table of calculation and experimental results studying deformation, displacement, total twisted angle on the shaft shows that the difference between the experimental results and the calculation is from 12 to 21%. Due to the complexity of the simulation and the calculation of propeller shaft, the above difference is acceptable.

Further research direction

Researchers propose further research direction to expand the hypotheses of propeller shaft in order to examine the effects on the durability of the propeller shaft such as: anti-torsional stiffness varying along the length of the shaft, tilt angle of the shaft in the horizontal plane with the impact of friction at the two bearings supporting the two ends of the shaft or horizontal bending moment of the shaft.

Continue to carry out experiment of the velocity and deformation of the propeller shaft assembly to supplement and complete theoretical studies.